College of Saint Benedict and Saint John's University

DigitalCommons@CSB/SJU

5-1-2011

Impact of dispersion on amplitude and frequency noise in a Yb-fiber laser comb

Lora Nugent-Glandorf

Todd A. Johnson
College of Saint Benedict/Saint John's University, toddjohnson@csbsju.edu

Yohei Kobayashi

Scott A. Diddams

Follow this and additional works at: https://digitalcommons.csbsju.edu/physics_pubs

Part of the Optics Commons

Recommended Citation

Nugent-Gladorf L, Johnson TA, Kobayashi Y, Diddams SA. 2011. Impact of dispersion on amplitude and frequency noise in a Yb-fiber laser comb. *Optics Letters* 36(9): 1579-1580.

Impact of dispersion on amplitude and frequency noise in a Yb-fiber laser comb

Lora Nugent-Glandorf,[1,*] Todd A. Johnson,[1] Yohei Kobayashi,[2] and Scott A. Diddams[1,3]

[1]National Institute of Standards and Technology, Time and Frequency Division, Mail Stop 847,
325 Broadway, Boulder, Colorado 80305, USA

[2]The University of Tokyo Institute for Solid State Physics, Kashiwanoha 5-1-5, Kashiwa, Chiba 277-8581, Japan

[3]e-mail: scott.diddams@nist.gov

*Corresponding author: LNG@boulder.nist.gov

We describe a Yb-fiber-based laser comb, with a focus on the relationship between the net-cavity dispersion and frequency noise on the comb. While tuning the net-cavity dispersion from anomalous to normal, we measure the relative intensity noise, offset frequency (f_{CEO}) linewidth, and the resulting frequency noise spectrum on the f_{CEO}. We find that the laser operating at zero net-cavity dispersion has many advantages, including an approximately 100× reduction in free-running f_{CEO} linewidth and frequency noise power spectral density when compared to the normal-dispersion regime. At the zero-dispersion point, we demonstrate a phase-locked f_{CEO} beat with low residual noise. © 2011 Optical Society of America

OCIS codes: 140.3510, 140.7090, 260.2030.

Yb-doped fiber femtosecond laser combs have been the subject of recent attention due to their high efficiency, high repetition rate capabilities, low noise, and ease of direct diode pumping and amplification [1–4]. Yb-fiber combs have proven particularly useful in spectroscopic applications, where amplification and nonlinear frequency generation can push the initial $1.03\,\mu m$ wavelength into the mid-IR [5,6] or ultraviolet [7]. There are several fiber laser designs [8] that can operate in various group delay dispersion (GDD) regimes, from soliton-like (net GDD is negative) to similariton pulse propagation (net GDD is normal). In all of these designs, net-cavity dispersion plays a significant role in the laser dynamics and must be carefully managed.

In order to explore the relationship between dispersion and amplitude and frequency noise on the frequency comb, we employ a laser design that can be tuned readily across a range of net-cavity dispersions. Because a frequency comb with low amplitude and frequency noise is necessary for precision spectroscopy and other applications, it is important to understand the properties of these Yb-fiber laser combs in all dispersion regimes. Noise on the comb teeth can originate from many different sources inside the cavity, including amplitude noise from the pump diode, amplified stimulated emission (ASE) jitter, cavity loss, and cavity length changes [9]. With a pair of volume holographic gratings, we are able to adjust the dispersion inside the cavity in order to study the dependence of the frequency comb noise on the net-cavity dispersion and to identify the optimum dispersion for obtaining a low-noise comb with narrow linewidth carrier-envelope offset frequency (f_{CEO}). In the time domain picture of frequency combs, f_{CEO} is the product of the repetition rate and the fractional carrier-envelope phase change ($\Delta\phi_{ce}/2\pi$) per cavity round trip. Noise on f_{CEO} can originate from noise on the repetition rate (timing jitter) or the carrier-envelope phase (phase jitter) [9–12], both of which are affected by the various noise sources in the system. The linewidth of f_{CEO}, while not the complete picture of noise in the laser system,

is a sensitive indicator of frequency noise when tuning the dispersion in the laser.

We have designed and built the Yb-fiber laser shown in Fig. 1 [1], where 70 cm of Yb gain fiber is pumped by a 976 nm laser diode (350 to 450 mW). The free-space section contains a polarizing beam splitter for output coupling, an isolator that promotes lasing in the correct direction, and a double pass through two volume holographic transmission gratings. The second grating can be translated a total of 1 cm, corresponding to a dispersion change of $16,000\,fs^2$ at a center wavelength of 1035 nm. Mode locking is initiated by careful movements of the three free-space wave plates. Depending on the mode-locking conditions, the laser output power ranges from 50 to 100 mW at a 100 MHz repetition rate. As is seen in the inset of Fig. 1, the optical spectrum varies considerably when changing the grating separation to tune the net-cavity dispersion of the laser from normal to anomalous.

To understand the effects of cavity dispersion on laser operation, it is first necessary to understand specifically what dispersion regimes are accessible. Determination of the actual cavity dispersion is not straightforward,
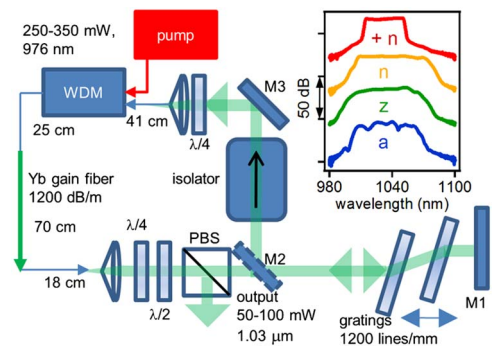

Fig. 1. (Color online) Schematic of Yb-fiber oscillator: WDM, wavelength division multiplexer; PBS, polarizing beam splitter; M1–M3, silver mirrors (M2 is a half mirror). Inset, optical spectra at four distinct dispersion regimes in the cavity (+n = more normal, n = normal, z = zero, a = anomalous).

because fiber dispersion curves (both Yb-doped and single mode) can vary significantly from manufacturing specifications and from fiber to fiber. Therefore, we first measured the cavity dispersion *in situ* using the technique of Knox [13]. By putting a slit that is narrower than the beam profile in front of the retroreflection mirror (M1 in Fig. 1), the optical spectrum, and thus the central wavelength of the mode-locked laser, can be scanned. The width of the mode-locked spectrum remains no less than 75% of the unfiltered spectrum. As the slit is scanned, the free-running repetition rate (f_{rep}) is monitored with a photodiode and recorded with a frequency counter. Differentiating the group delay, $T_g(= 1/f_{rep})$ versus the center frequency of the optical spectra (ω_0) yields the net-cavity GDD. The experimental results for four grating separations are shown in Fig. 2 (circles). The solid lines in Fig. 2 are the calculated dispersion based on the sum of the elements inside the cavity, including reasonable estimates of fiber dispersion (Yb fiber estimate from [14] and SMF from FLEX 1060 fiber data), dispersion from high-refractive-index materials (glass optics and terbium gallium garnet [15], a material found in optical isolators), and grating dispersion [16]. The results show that the four mode-locked spectra in the inset of Fig. 1 correspond to one anomalous, one near-zero, and two normal-dispersion regimes. While third-order dispersion is evident in the slope of the lines in Fig. 2, we define the net-cavity GDD (from normal to anomalous) using the second-order dispersion value at the nominal center wavelength (1035 nm for all spectra in Fig. 1).

With a clear understanding of the cavity dispersion, we measured the free-running offset frequency, f_{CEO}, of the laser operating in several dispersion modes. To this end, we first amplified the chirped oscillator output in a core-pumped Yb-doped fiber amplifier then recompressed the pulses with an external double-pass grating pair (average power ~400 mW, 80 fs pulse duration). Continuum generation was achieved with a 15 cm piece of nonlinear suspended-core fiber [17]. An f_{CEO} beat was then measured with a standard f-2f interferometer [18]. The microwave spectra of two sample f_{CEO} beat signals are shown in Fig. 3(a) for the normal- and zero-dispersion regimes, illustrating the significant difference in linewidth. Similar effects have been observed in other Er and Yb laser systems [19]; however, to our knowledge, this dependence has not been mapped over a range of cavity dispersions.

A complete set of measurements of the free-running f_{CEO} linewidth versus dispersion is given in Fig. 3(b). A clear trend of decreasing f_{CEO} linewidth toward zero
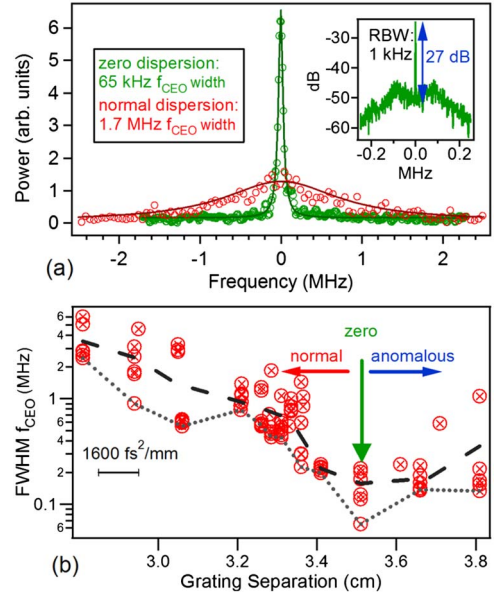
Fig. 3. (Color online) (a) Spectrum of free-running f_{CEO} beat at normal- and zero-dispersion points with Lorentzian fits. Inset, locked f_{CEO} beat. (b) Collection of f_{CEO} linewidths versus net-cavity dispersion (measured by grating separation): dotted curve, minimum linewidth obtained and dashed curve, average value.

dispersion (from both the normal and anomalous sides) is seen. For each dispersion regime (i.e., a fixed grating separation), the f_{CEO} linewidth can also change with pump power (which directly affects the internal cavity circulating power and the spectral width of the pulse). At each grating separation, the pump power was tuned within the full range of stable mode locking (i.e., no cw breakthrough). Many factors, including the pumping rate, cavity loss, and the laser's nonlinear response can impact the f_{CEO} linewidth, including the "turning points" [20] of the f_{CEO} beat and the polarization settings. Nevertheless, in the normal-dispersion mode, we never obtained an f_{CEO} linewidth as narrow as in the zero-dispersion regime.

As the microwave power spectrum [Fig. 3(a)] can ambiguously mix amplitude and frequency noise, we also directly measured the frequency noise spectrum of f_{CEO}. This was accomplished by sending the f_{CEO} beat signal into a frequency divider followed by a delay line discriminator and a vector signal analyzer. These results are given in Fig. 4(a) for laser operation at normal and zero dispersion, corresponding to measured free-running f_{CEO} widths of 1.45 MHz and 130 kHz, respectively. The broad f_{CEO} beat clearly has considerably higher FM noise. Calculation of rf spectra from the frequency noise spectra in Fig. 4(a) (using numerical methods) yields a FWHM of 1.50 MHz (normal) and 104 kHz (zero), a correspondingly 3% and 20% deviation from the experimental values. This might suggest a small contribution from AM noise in the zero-dispersion regime, while the much higher FM noise in the normal regime masks any AM contribution. Nonetheless, it is clear that the frequency noise dominates the f_{CEO} linewidths. It is also possible to tightly lock the f_{CEO} beat in the zero-dispersion regime, as shown in the inset of Fig. 3(a), where the coherent signature on a undivided copy of f_{CEO} (at 226 MHz) is seen.
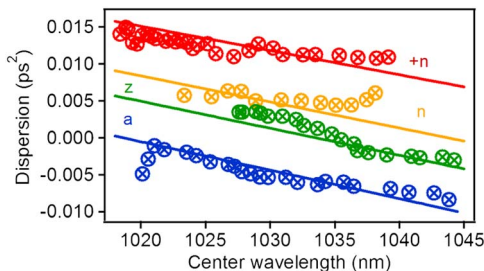

Fig. 2. (Color online) Experimental measurement of the laser cavity GDD (circles) and calculation of dispersion as a sum of all the cavity elements (solid lines).
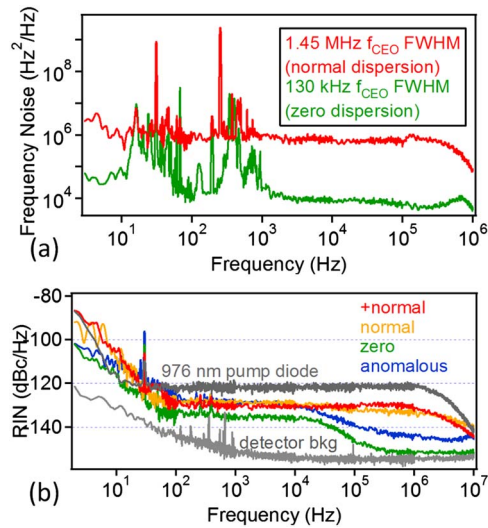
Fig. 4.   (Color online) (a) Frequency noise on two sample f_{CEO} beat signals (division factor included to give true f_{CEO} noise). (b) Amplitude noise (RIN) for four dispersion regimes.

In this spectrum, 90% of the power is located within the coherent carrier.

In most frequency combs, there is a strong coupling between amplitude and frequency noise. The amplitude noise of the laser oscillator was measured [Fig. 4(b)] at the same four net-cavity-dispersion regimes shown in Figs. 1 and 2. Amplitude noise was measured by monitoring a portion of the laser output with a fast photodiode (1 GHz bandwidth) and using a vector signal analyzer to obtain a power spectral density of the relative intensity noise (RIN = $[\Delta P_{rms}/P_o]^2$ per Hz bandwidth, where P is the optical power). We observed significant differences in the RIN as a function of net-cavity dispersion, with zero net-cavity dispersion having the lowest RIN. It is not possible to state that "all other parameters are equal" except the dispersion when comparing the different laser operating modes. Each dispersion point requires adjustment of the pump diode power and waveplate settings in order to achieve stable mode locking, leading to differences in output coupling and cavity Q. However, in practice, the zero-dispersion mode consistently shows the lowest RIN. We also present the pump laser RIN in Fig. 4(b). The white-noise level of the pump RIN is nearly constant with the changing pump current (data not shown), and it is on average 10 dB higher than the oscillator RIN.

Experimentally, the Yb-fiber oscillator presented here operates in its quietest mode near zero dispersion, including reduced amplitude noise on the oscillator, narrowest f_{CEO} linewidth, and less frequency noise on f_{CEO} itself. This fact alone should be important for the further development of such lasers for frequency comb applications. Additionally, it is interesting to note that our measurements of f_{CEO} noise are consistent with the prediction of minimum timing jitter for stretched-pulse fiber lasers near zero net-cavity dispersion [9,21]. This could imply a direct correlation between noise on f_{CEO} and f_{rep}, where ASE-induced center wavelength changes are coupled to timing jitter through the group velocity dispersion [9,10,21]. However, the connection between various noise sources and the frequency noise

on the comb itself can be complicated [9,12,21,22], and direct measurements of the timing jitter would help provide a more complete picture of the noise properties of Yb-fiber laser combs [23].

References

1. X. Zhou, F. Yoshitomi, Y. Kobayashi, and K. Torizuka, Opt. Express **16**, 7055 (2008).
2. T. Schibli, I. Hartl, D. Yost, M. Martin, A. Marcinkevičius, M. Fermann, and J. Ye, Nat. Photon. **2**, 355 (2008).
3. M. Fermann and I. Hartl, IEEE J. Sel. Top. Quantum Electron. **15**, 191 (2009).
4. I. Hartl, L. Fu, B. Thomas, L. Dong, M. Fermann, J. Kim, F. Kartner, and C. Menyuk, in *Conference on Lasers and Electro-Optics/Quantum Electronics and Laser Science Conference and Photonic Applications Systems Technologies*, OSA Technical Digest (CD) (Optical Society of America, 2008), paper CTuC4.
5. F. Adler, K. Cossel, M. Thorpe, I. Hartl, M. Fermann, and J. Ye, Opt. Lett. **34**, 1330 (2009).
6. T. Johnson and S. Diddams, in *Conference on Lasers and Electro-Optics*, OSA Technical Digest (CD) (Optical Society of America, 2010), paper CPDB11.
7. D. Yost, T. Schibli, J. Ye, J. Tate, J. Hostetter, M. Gaarde, and K. Schafer, Nat. Phys. **5**, 815 (2009).
8. F. Wise, A. Chong, and W. Renninger, Laser Photon. Rev. **2**, 58 (2008).
9. N. Newbury and B. Swann, J. Opt. Soc. Am. B **24**, 1756 (2007).
10. J. Gordon and H. Haus, Opt. Lett. **11**, 665 (1986).
11. O. Prochnow, R. Paschotta, E. Benkler, U. Morgner, J. Neumann, D. Wandt, and D. Kracht, Opt. Express **17**, 15525 (2009).
12. B. Washburn and N. Newbury, IEEE J. Quantum Electron. **41**, 1388 (2005).
13. W. H. Knox, Opt. Lett. **17**, 514 (1992).
14. L. Grüner-Nielsen, S. Ramachandran, K. Jesperen, S. Ghalmi, M. Garmund, and B. Palsdottir, Proc. SPIE **6873**, 68730Q (2008).
15. U. Sugg and B. Schlarb, Phys. Status Solidi (b) **182**, K91 (1994).
16. A. M. Weiner, *Ultrafast Optics* (Wiley, 2009).
17. L. Dong, B. K. Thomas, and L. Fu, Opt. Express **16**, 16423 (2008).
18. D. Jones, S. Diddams, J. Ranka, A. Stentz, R. Windeler, J. Hall, and S. Cundiff, Science **288**, 635 (2000).
19. N. Kuse and Y. Kobayashi, The University of Tokyo Institute for Solid State Physics, Kashiwanoha 5-1-5, Kashiwa, Chiba 277-8581, Japan; I. Hartl, IMRA America, 1044 Woodridge Avenue, Ann Arbor, Michigan 48105, USA (personal communication, 2010).
20. K. Holman, R. Jones, A. Marian, S. Cundiff, and J. Ye, Opt. Lett. **28**, 851 (2003).
21. S. Namiki and H. Haus, IEEE J. Quantum Electron. **33**, 649 (1997).
22. H. Telle, B. Liphardt, and J. Stenger, Appl. Phys. B **74**, 1 (2002).
23. Y. Song, K. Jung, and J. Kim, arXiv:1102.1046v1 (2011).